

CHAPTER 145

LOADING AND RESPONSE OF CYLINDERS IN WAVES

by G N Bullock¹, P K Stansby¹ and J G Warren²

1. Introduction

The nature of the wave-induced flow around a circular cylinder is to a large extent determined by the ratio of water-particle orbit size to cylinder diameter, characterized in regular waves by the Keulegan-Carpenter number KC (see Appendix II for definitions). When $D/L > 0.2$ wave scattering effects are negligible and it is conventional to describe the fluid loading in terms of drag and inertia forces in-line with the direction of wave propagation plus a transverse 'lift' force.

The idealised two-dimensional situation of a cylinder normal to planar sinusoidal flow has been investigated in U-tubes by Sarpkaya (10, 11). As KC advances above 2 vorticity starts to be shed and produces forces in addition to the inertia force which would result from the undisturbed fluid acceleration. The vortex-induced forces become more important as KC increases. Defining the drag force as the component of the in-line force in phase with the fluid velocity and the inertia force as the component in phase with the acceleration, it is found that the drag, inertia and lift can have comparable magnitudes when KC is between 8 and 25. This paper is concerned with the corresponding regime in waves.

In the idealised situation vortex shedding is almost perfectly correlated along the length of the cylinder but generally this will not be the case in waves. Here the degree of vortex coherence will influence the vortex-induced forces particularly the lift which is strongly dependent on history effects. Although the forces on fixed vertical cylinders have been measured, little is known about the loading on cylinders in general orientation in either unidirectional waves or planar flows. Real seas are further complicated by being random and multidirectional with the possibility of superimposed currents. The interaction of cylinder vibration with vortex shedding can be highly non-linear in currents, e.g see (12), but again little is known about what happens in waves.

Although scale influences the magnitude of forces when vortex shedding is important, small-scale experiments can qualitatively represent full-scale flows. Thus, the interrelation between the various parameters which influence wave loading may be studied in the relatively controlled environment of a laboratory channel. Furthermore, analysis techniques which have been justified on the model scale can then be applied with greater confidence to full-scale situations.

1. Civil Engineering Department, University of Salford, England
2. Taylor Woodrow Construction Ltd. London, England.

In this paper we consider the loading and response of small-diameter flexible cylinders with natural frequencies of vibration in excess of the dominant wave frequency. The way in which vortex shedding generates loading is illustrated by results from a mathematical model (13) and a brief review of experimental studies using fixed cylinders. This is followed by a description of an investigation in which flexible cylinders were mounted as vertical cantilevers in a laboratory wave channel. Both regular and 'random' waves were generated while structural frequencies were tuned through a range of values. Methods of predicting the in-line response are tested and the cross-flow response is evaluated.

With the test cylinder in regular waves, in-line and transverse displacements at still water level, x_0 and y_0 , depend upon

$$f_w, D, \rho, \mu, f_n, S_n, \bar{m}, \delta, t, k, d$$

Dimensional analysis gives

$$\frac{x_0}{D}, \frac{y_0}{D} = f\left(KC, Re, kd, \frac{S_n}{d}, \frac{t}{T}, \delta, \frac{\bar{m}}{\rho D^2}, Fr\right)$$

where the Reynolds number (Re) is effectively a scale parameter. In planar oscillatory flows the parameter kd , which indicates the degree of particle motion attenuation with depth, and S_n/d , which indicates the degree of wave non-linearity, both disappear.

2. Vortex Shedding in Planar Oscillatory Flows

A mathematical model of two-dimensional vortex shedding from the circular cylinder has been developed (13). Principles of potential flow are used and the separating shear layers are represented by discrete vortices. Fixing separation on the line through the cylinder centre normal to the incident velocity gives forces which are in reasonable agreement with experiment (11) at very high Reynolds numbers for $KC > 12$ (approx.). Fig. 1 shows the variation of non-dimensional in-line and lift force, $C_x(t)$ and $C_L(t)$, with time for $U = U_0 \cos(2\pi t/T)$ and $KC = 12.5$ and 18.4 . The in-line force is closely predicted by Morison's formula, $\frac{1}{2}\rho DU|U|C_D + \frac{1}{2}\rho\pi D^2 \dot{U}C_M$ with $C_D = 0.7$ and $C_M = 1.4$, even though there are complex asymmetric vortex motions which cause lift fluctuations at higher frequencies than the incident flow frequency. These vorticity patterns are sketched in Fig. 2 for $2.25 < t/T < 2.75$. The vorticity is concentrated in areas rather than at points.

The lift variations are not repetitive for the examples shown although nearly periodic forms have been observed in certain cases. This is in keeping with experimental studies at low Reynolds numbers (8). Fig. 2 shows that for $KC = 12.5$ the strong positive vortex shed in the previous half cycle moves towards the cylinder generating positive lift at $t/T = 2.25$ and 2.35 . At $t/T = 2.45$ positive vorticity rolling

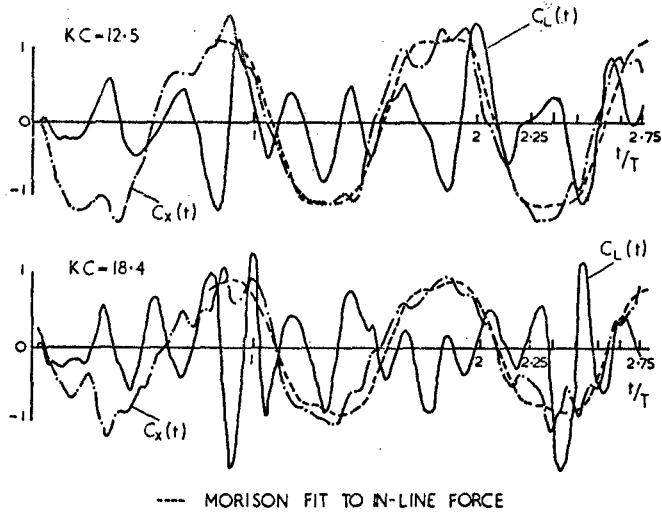


Fig. 1. Time histories of $C_x(t)$ and $C_L(t)$ from mathematical model

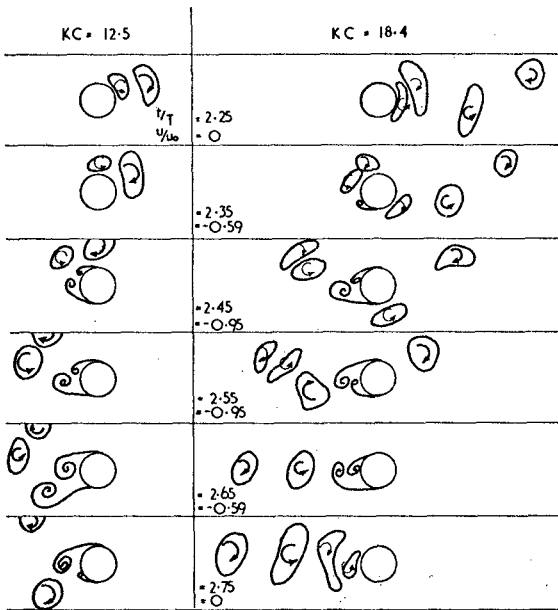


Fig. 2. Sketches of vortex movement to demonstrate generation of forces.

up close to the cylinder generates negative lift. At $t/T = 2.55$ and 2.65 negative vorticity rolling up close to the cylinder generates positive lift. By $t/T = 2.75$ two lumps of vorticity have been shed corresponding to those at $t/T = 2.25$. For $KC = 18.4$ the situation is similar, the four vortices shed causes four peaks in lift with an initial peak from the returning vorticity of the previous half cycle. The vorticity from earlier half cycles appears to have little effect. The rule that the ratio of lift frequency to flow frequency is $N + 1$ where N is the number of vortices shed per half cycle is thus demonstrated. However the rule does not always apply, particularly when N is large and the shed vortices vary considerably in strength.

3. Fixed Vertical Cylinder in Waves

Various investigators have measured wave forces on fixed vertical cylinders in laboratory wave channels. C_D and C_M have been calculated (using horizontal water-particle motions from third order wave theory) for a section close to the surface (9) and C_D values were found to be slightly greater than for planar oscillatory flows (10) with $10 < KC < 25$. Other tests (14) indicate that the use of C_D and C_M from U-tube experiments will give a good representation of local in-line forces.

Local lift forces have also been measured (2) and their Fourier components were found to be dependent on spanwise position. A non-uniform velocity distribution has been investigated in detail for a steady flow approaching a circular cylinder (7). The linear spanwise velocity variation caused vortex shedding, and hence lift frequencies to be roughly proportional to local velocity although these frequencies would be unchanged for several diameters as vortices were shed as distinct 'cells'. Thus vortex lines were not continuous throughout the depth. Such incident flows contain vorticity normal to the cylinder axis while waves are essentially irrotational. But a uniform, and hence irrotational flow incident on a tapered cylinder also produced cells of different frequency (4). It seems likely that incoherent cell structure will also occur in waves, at least when several vortices are shed per half cycle.

Lift fluctuating mainly at the wave frequency has been measured for $KC < 5$ (2) and this has not been observed in planar or other wave flows (to the writers' knowledge). This could however be due to wave non-linearity effects as vortex patterns due to the passage of a wave crest can be very different from those due to the passage of a trough (16). Local C_D and C_M values were also calculated in (2) and the high degree of scatter could in part be due to the use of linear wave theory. For $6 < KC < 14$ lift at almost entirely twice the wave frequency is in agreement with Isaacson and Maull (5) who measured the total force on the cylinder. However differences in magnitude may again be due to different non-linearity effects. For $KC > 16$ the rms lift has decreased (5) and contains several Fourier components of similar magnitude.

4. Flexible Vertical Cylinder in Waves

The present investigation was conducted in a 1.25m wide x 0.8m deep x 40m long laboratory channel with a computer-controlled, piston-type paddle at one end and a gently sloping, 10m long, 'beach' at the other (Plate 1). The beach was estimated to have a reflection coefficient that varied from 2.8% up to 5.0% over the range of wave frequencies considered. The temporal variation in water surface elevation was measured by capacitance-type wave gauges linked to the computer which was used for data collection and some analysis.

When regular waves were required the computer was programmed to adjust a sinusoidal paddle motion until waves with a specified frequency and standard deviation of water surface elevation were generated at the test section. A system was developed whereby data of the type presented in Fig. 3 could be automatically collected for up to 48 different wave conditions. 'Random' waves were generated by the use of an algorithm (3) in which pseudo-random noise is produced by feedback in a shift register and passed through a digital filter to give the paddle motion for the desired wave spectrum. Because this technique produces a deterministic time series it is possible to conduct a series of tests in nominally identical wave conditions.

Four 0.8m long cylinders with diameters ranging from 21mm to 54mm were used in the investigation (see Table 1). When a particular cylinder was under test it was mounted on the bottom of the channel in a 0.6m depth of water to form a vertical surface-piercing cantilever. The required degree of flexibility was achieved by fabricating each cylinder from Polypropylene tube (Young's Modulus of 700 MN/m^2) and the resonant frequency was controlled by use of a variable tip mass. Vibration was measured by means of two pairs of strain gauges positioned 25mm above the base and displacements were estimated on the basis of the first mode shape. Negligible motion was detected at frequencies associated with any higher mode.

The logarithmic decrements of structural damping were determined in free vibration tests to be between 0.18 and 0.22. The mass of each structure was generalised by use of an equivalent mass (\bar{m}) defined in the way that has become standard for estuarial structures. Thus \bar{m} is the mass/unit length of a uniform cylinder extending to mean water surface level which vibrates with the same energy, resonant frequency and mode shape as the original structure. Values of f_n were determined in still water tests. A particular test structure was then defined by means of the dimensionless parameters Fr , δ and $\bar{m}/\rho D^2$.

Regular Wave Tests

These tests were carried out with intermediate depth waves ($0.5 < kd < 3.0$) at surface Re between 4.6×10^3 and 17×10^3 and KC up to 28, all values calculated using linear theory.



Plate 1. General view of experimental equipment.

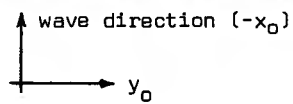
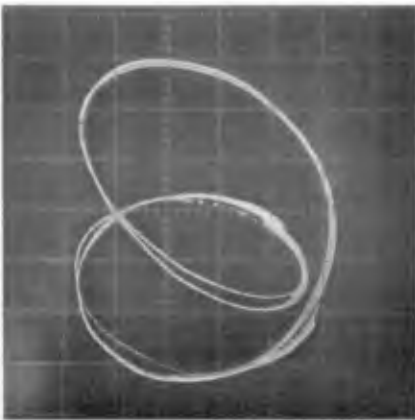


Plate 2. Oscilloscope traces of the temporal variation in x_0 and y_0 during series A test with $Fr = 2.0$ and $KC = 17$.

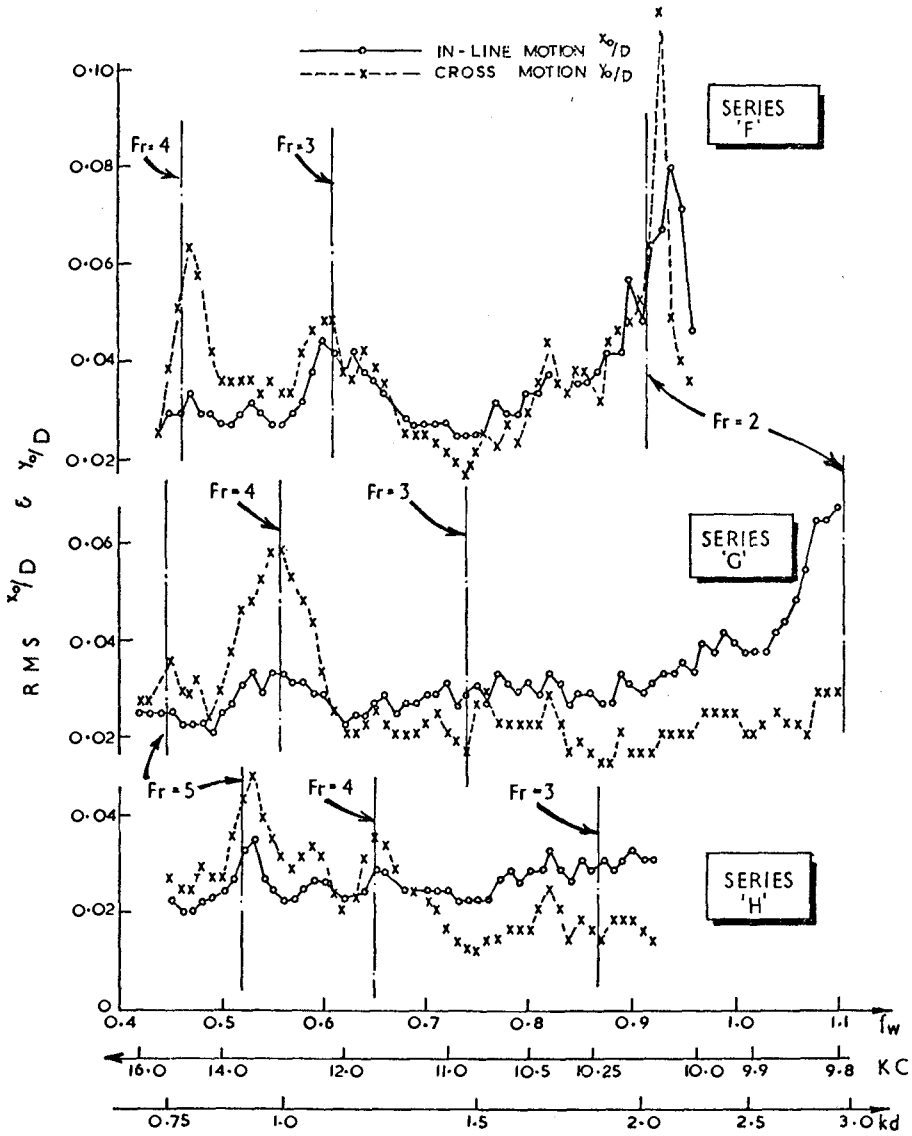


Fig. 3. Typical results for the variation in root-mean-square x_0/D and y_0/D against various parameters for regular waves.

Fig. 3 shows three typical sets of results for the variation in rms x_0/D and y_0/D against Fr , KC and kd . Additional parameters for these and other similar tests are given in Table 1. Because cross-flow response was often quite different from one wave cycle to the next, each point in Fig. 3 is based on 19,600 readings taken at 0.06 sec intervals (350 to 1300 wave cycles) to give sensible statistical estimates. For the range of parameters considered the cross-flow response can be much greater than the in-line response and both motions tend to increase as Fr approaches an integer value. The wave height for the runs in Fig. 3 was unchanged at 113mm. (The low level of reflection is considered to have little influence on the results).

The in-line response followed a very similar pattern in each wave cycle of a particular test but the form of the pattern depended upon the prevailing test parameters. Several attempts were made to predict the observed behaviour. In these the cylinder was divided into segments and the horizontal water-particle motion at the centre of each segment was calculated from simple theory. Local KC values were used in conjunction with data from U-tube experiments (10) to assign values to C_D and C_M in the Morison equation and hence to estimate the bending moment at the cylinder base. Wave-induced motion was predicted by assuming that the cylinder formed part of a linear, single-degree-of-freedom system and feeding a time series of base bending moments into a finite difference scheme based on the appropriate equation of motion. The best results were obtained when the Morison equation was extended to include relative motion terms, when some account was taken of the variation in water-surface elevation and when second order rather than first order wave theory was used. Fig. 4 shows a comparison of measured and predicted time-histories for base strain while Fig. 5 shows a more general comparison of rms x_0/D values. The predictions were good except when $Fr \approx 2$ and the experimental cylinder was subjected to strong transverse bending moments that varied at twice the wave frequency. In these circumstances, which occurred when the surface KC was around 13, the observed in-line motion was seriously underestimated.

The general success of the extended Morison equation when used with coefficients obtained with stationary cylinders suggests that the vorticity shed in a wave cycle is mainly dependent on the relative in-line fluid motion. However, in these experiments the cylinder motion was always small in comparison with the fluid motion. If we assume that the vorticity shed was largely independent of response, because vorticity was mainly responsible for in-line motion and entirely responsible for cross motion, it is reasonable to expect rms $y_0/rms x_0$ to be sensibly constant for situations with the same Fr , KC and kd . Further specification by $\bar{m}/\rho D^2$ and δ is conveniently avoided as they affect only the magnitude of the responses and S_n/d was the same in most tests. In the present case KC was a more important parameter than kd , so ratios of rms $y_0/rms x_0$ were calculated from the experimental results and plotted against Fr and KC . This produced a chart similar to Fig. 6 in which each dot indicates the location of a

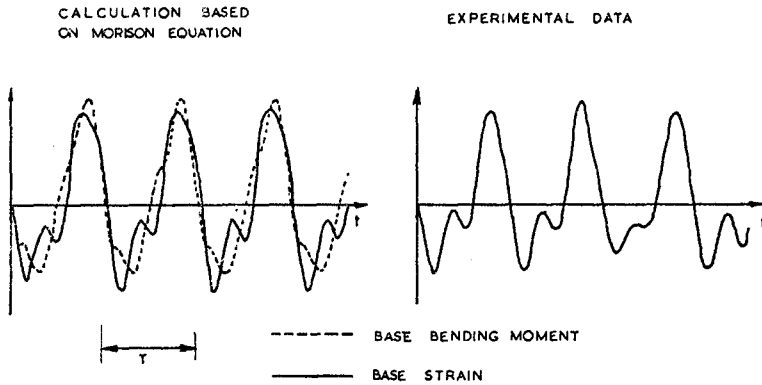


Fig. 4. Time histories of base bending moment and strain
 $Fr = 2.4$ $KC = 13.9$ $kd = 1.54$

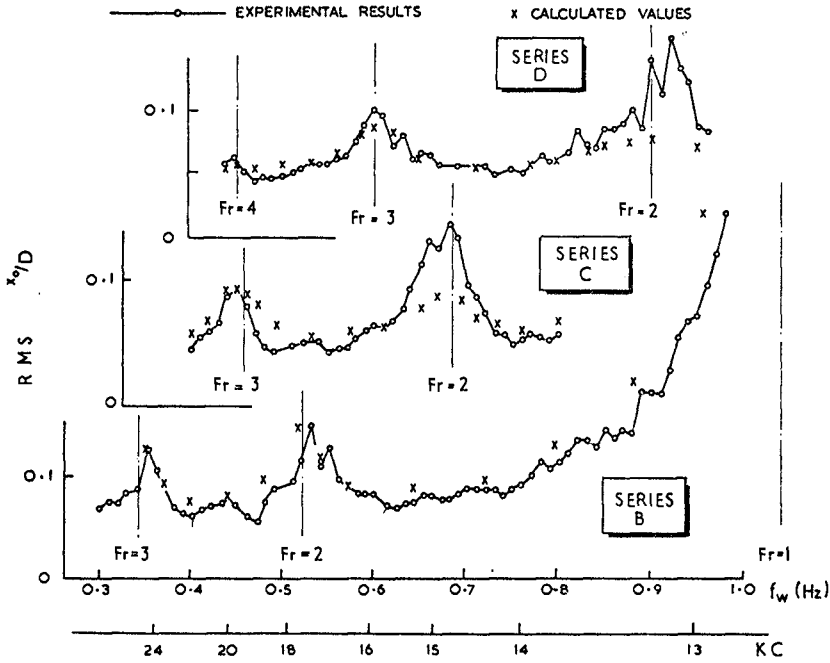


Fig. 5. Comparison of experimental and calculated values for root-mean-square x_0/D .

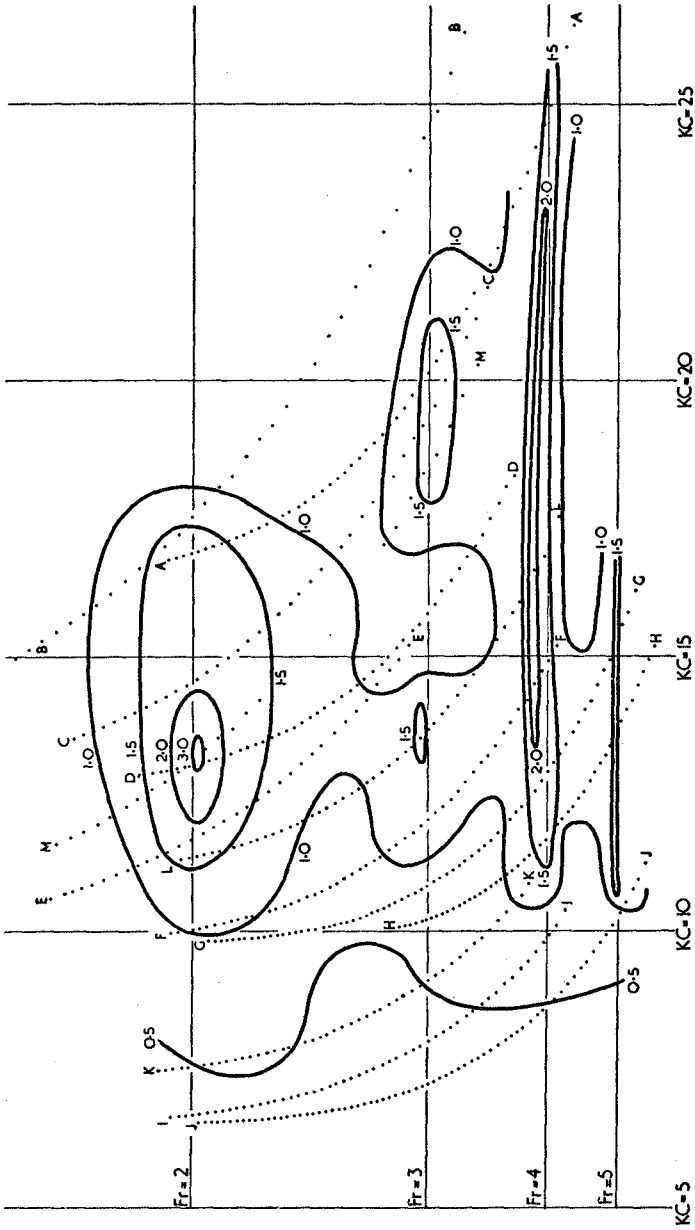


Fig. 6. Contours of $\text{rms } y_0/\text{rms } x_0$ against Fr and KC. Each dot indicates the location of a result from the series of tests A to M detailed in Table 1.

result from the series of tests A to M detailed in Table 1. (In each test k_d decreased from about 2.5 to 0.75 with increasing KC). The scatter in the values of $\text{rms } y_0 / \text{rms } x_0$ found within a given region of the chart was small enough (15) to justify the sketching of contours as shown. Values in excess of 3 were obtained only in the sensitive area around $Fr = 2$ and $KC = 13$ where the vorticity shed in a wave cycle was probably markedly dependent on response (see § 5).

Unlike the in-line motion, the transverse response tended to be very erratic with intermittent bursts of activity that varied in both magnitude and duration. However, during tests in which f_n was close to the frequency of a major component in the transverse bending moment, y_0 would occasionally follow repetitive patterns which could persist for many wave cycles. The most stable responses were generally associated with the sensitive area around $Fr = 2$ and $KC = 13$. When these broke down either the same pattern or its mirror image in the in-line plane was quickly re-established (Plate 2).

Some characteristics of the different types of motion are illustrated by the probability density histograms shown in Fig. 7, the right hand pair being for the conditions of Plate 2. The in-line histograms are asymmetric, mainly due to the different loading produced by the passage of wave crests as opposed to troughs, whereas the transverse histograms are symmetric. Because the cross motion varies from the very erratic to the near sinusoidal oscillations associated with a repetitive pattern, the corresponding probability density histograms are a combination of the 'bell-shaped' Gaussian and two-peaked, sine-wave density functions. The relative magnitudes of these forms within a particular histogram give an indication of the periods over which the different conditions were prevalent. Spectral analyses of both the in-line and transverse response show the variance to be mainly at harmonics of f_w , significant dynamic magnification occurring whenever f_n was close to a wave harmonic. A fair proportion of the in-line response always occurred at f_w but this was not true of the transverse motion.

Time-histories of in-line and transverse base bending moments were calculated from strain data for 82 seconds of selected tests. As would be expected spectral analyses reveal that most of the variance in the in-line moment occurred at f_w whereas the largest harmonic in the transverse moment depended upon the prevailing test parameters. An indication of the regions over which various harmonics predominate is shown in Fig. 8 which suggests that the boundary between adjacent regions moves towards higher KC as k_d increases. This is doubtless due to the increasingly non-uniform velocity distribution as one moves towards a condition of 'deep-water' waves. In these circumstances the local value of KC reduces with depth and it is quite possible for the dominant harmonic in the transverse loading near the surface to have higher frequency than that of the dominant harmonic in the loading further down (2).

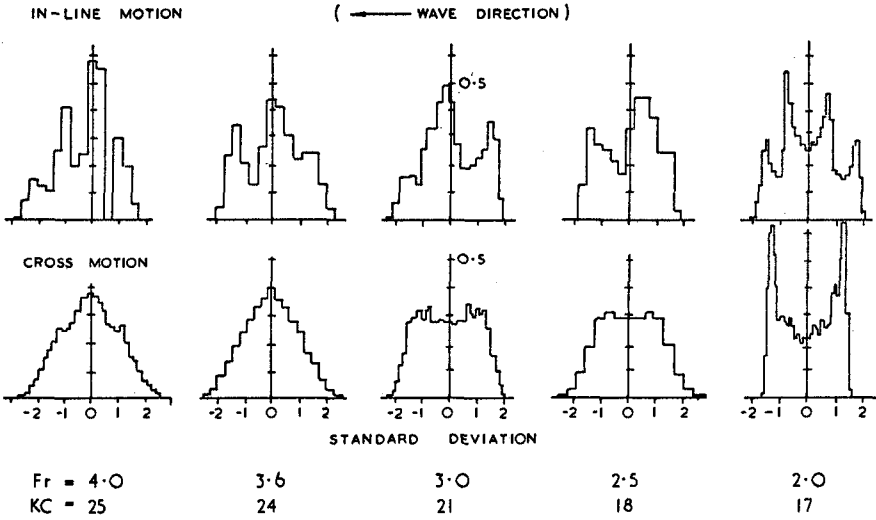


Fig. 7. Probability density histograms for structural motion in selected series A tests.

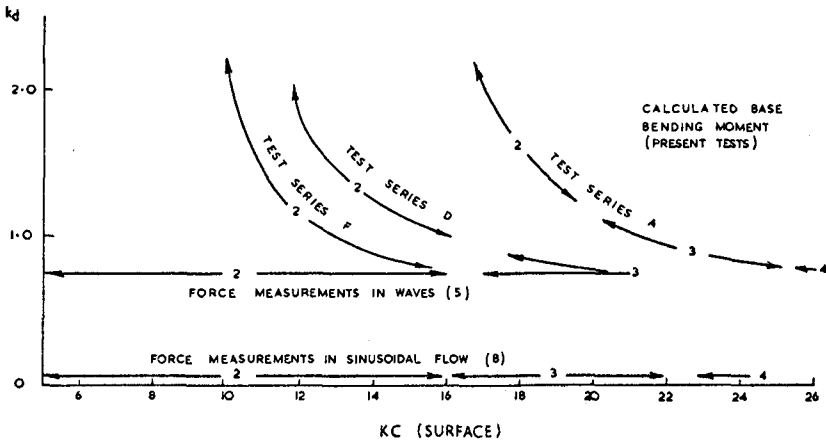


Fig. 8. Predominant harmonic in transverse moment or force

Random Wave Tests

During these tests the waves had a Pierson-Moskowitz spectrum with $S_{\eta} = 32\text{mm}$ and the variation in water-surface elevation was approximately Gaussian. Spectra for in-line and transverse response of the 28mm diameter cylinder when tuned to various f_n above the frequency of the wave spectral peak are shown in Fig. 9.

In most tests the in-line motion was dominated by vibration at the natural frequency although there was always significant response at frequencies associated with the peak of the wave spectrum. The spectral peak at f_n rapidly diminished as f_n was increased.

Predictions of in-line response were made in the frequency domain by applying transfer functions to the measured wave spectrum. The effects of structural movement were ignored so that base bending moment spectra could be calculated by use of linear wave theory and a linearised drag term in the Morison equation as proposed by Borgman (1). Guidance in the choice of values for the Morison coefficients was sought by calculating surface KC values for a regular wave with the same S_{η} as the wave spectrum and a frequency equal to that of the spectral peak. For the situation of Fig. 8 this gave $KC = 14$. U-tube experiments (10) indicate that around this value $C_D \approx 2$ and $C_M \approx 1$ and for simplicity these values were assumed to apply throughout the water depth. The response spectra obtained from the bending moment spectra by use of appropriate dynamic admittance terms were in remarkably close agreement with the experimental results (e.g Fig. 9). This is perhaps surprising as the calculations were drag-dominated and suggests that the errors inherent in the assumptions must at least partially cancel each other out. Refinement of the present calculations was not justified and new tests will be carried out to investigate this matter further.

The transverse response was of comparable magnitude to the in-line response but occurred only at frequencies near f_n . It was highly irregular and tended to be dominated by short bursts of above average motion which appeared to be either caused by the passage of a single wave or built up by a sequence of waves. Short bursts of high response at f_n also occurred in the in-line direction but did not necessarily coincide with those in the cross mode. Examination of the limited number of spectra obtained for the transverse response indicated that the variance did not always decline when f_n was increased. Instead there was a suggestion that the response increased when f_n was near an integer multiple of the dominant wave frequency in a manner reminiscent of the regular wave tests. It is interesting to note that the situation with $KC = 11$ and $Fr = 3.8$ occurred in both regular and random waves and the rms y_0 values were very similar (KC and Fr for random waves were calculated on the basis of a sine wave as previously described).

5. Analysis

The experiments were primarily concerned with the evaluation of response

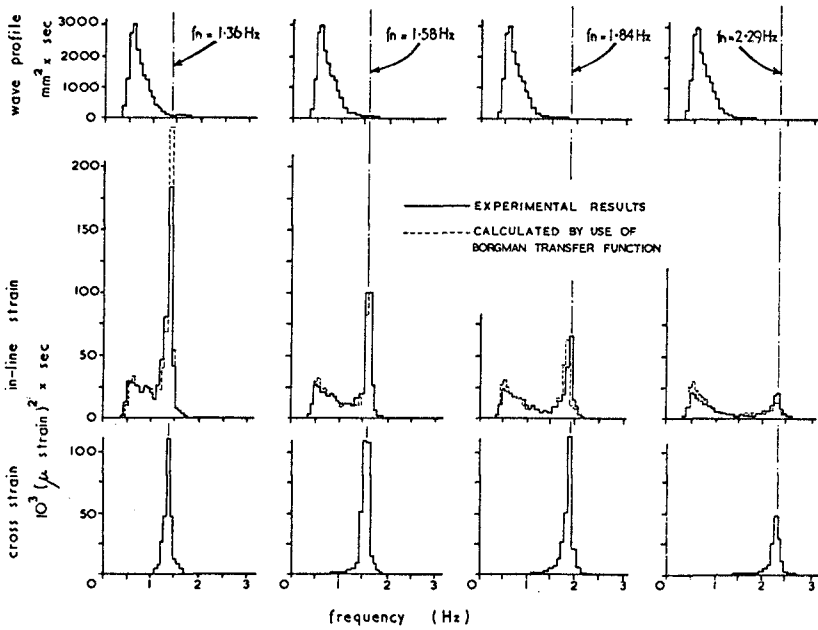


Fig. 9. Response of 28mm diameter cylinder in random waves.

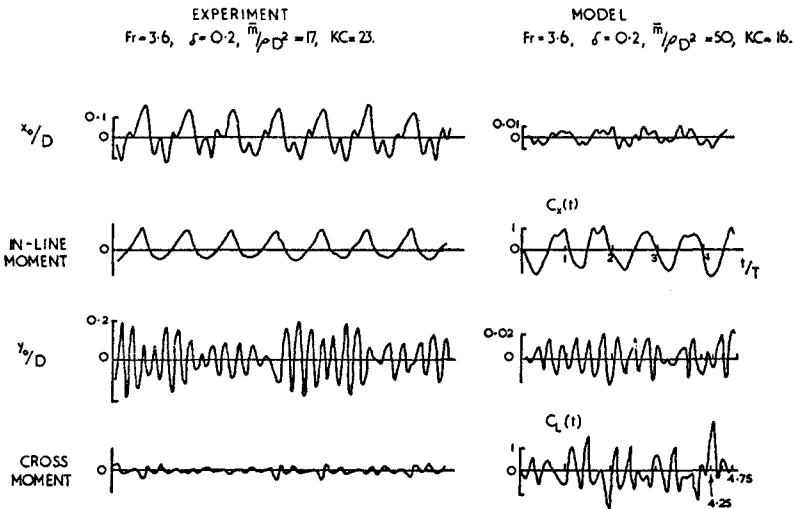


Fig. 10. Comparison of experimental results with results from the two-dimensional mathematical model

due to vortex shedding in waves. In regular waves definition of water-particle motions in an accepted manner together with the use of Morison's equation with relative motion terms and coefficients for fixed cylinders usually gave a good prediction of in-line response. This prediction was not disrupted by cross response which was often greater than the in-line response. An equivalent prediction method does not exist for cross motion and $\text{rms } y_0/D$ should ideally be defined by all the stated non-dimensional groups. To avoid this an approximate argument, which assumes that vorticity shed in a wave cycle is independent of the response which it generates, allows $\text{rms } y_0/\text{rms } x_0$ to be defined in terms of Fr , KC and kd . The contour plot of Fig. 6 is itself a justification for its method of presentation. The influence of kd is however omitted and Fig. 9 shows its effect on the dominant frequency of lift moment. This will affect the dependence of cross response on KC . It may be possible to weight KC through kd to overcome this.

The in-line response is underestimated by the above prediction for parameters approximately given by $1.8 < Fr < 2.2$ and $10 < KC < 17$. The area acceptably fits the contour plot and $\text{rms } y_0/\text{rms } x_0$ attains a maximum of 3. Lift moment is predominantly at twice the wave frequency and cross response and moment are at their most repetitive. Because drag and lift are vortex-induced it seems likely that the strength of the one vortex shed per half cycle is usually magnified by the response. This is analogous to the situation in currents where cross motion increases the vortex-induced forces which then increase the response in a feedback loop until equilibrium is reached, e.g see (12). The lift also 'locks-on' to the cylinder motion. However in waves, outside the sensitive area, cross response appears to have little influence on the vortex-induced forces in a permanent or long-term sense. Experiments with a linear mode response (6), which covered a range of δ , support this although the sensitive area was not found.

Cross response never defines the lift moment frequency and without this stabilising influence apparently stable patterns will always break down. In general cross response and moment are irregular and their fine structure is obviously interactive. Such patterns are shown in Fig. 10 and compared with the two-dimensional mathematical model. The potential-flow calculation accommodates cylinder velocities but only very small responses are considered because of the assumption of fixed separation. The KC of the high Reynolds number simulation is adjusted to give the same lift frequencies as the surface KC in waves. The different $\bar{m}/\rho D^2$ cause the model response to be roughly 1/10 of the experimental response but the interaction is similar for both. Lift acting against the motion reduces response while lift acting with the motion increases it. For the mathematical model the peak lift was greater than on the fixed cylinder but rms values were similar. It is important to note that in the experiment the small lift moment causes a greater response than the much larger in-line moment. The peaks in lift moment are considerably smaller than would be obtained by dividing the span into segments and summing the influence of lift maxima obtained from U-tube experiments through the associated KC values.

Extension of these results to other situations requires an interpretation of the physical processes involved. Magnification of vortex-induced forces by response is most likely when forces and response are nearly sinusoidal and at the same frequency (the situation of locking-on in steady currents). When the force is complex with spectral analysis indicating several harmonics of similar magnitude, feedback through a response at around the natural frequency would have to have a remarkable form to magnify the force in a permanent way.

Random waves will further reduce the possibility of permanent magnification and rms cross response can be as large in random waves as it is in regular waves for the same S_n and K_C . The prediction of in-line response in the frequency domain by making several assumptions was remarkably good. However the validity of each assumption should be checked in isolation.

APPENDIX I - References

1. Borgman, L E "The Spectral Density of Ocean Wave Forces". Coastal Engineering, ASCE Specialty Conference, Santa Barbara, October 1965, pp 147-182.
2. Chakrabarti, S K, Wolbert, A L, and Tam, W A "Wave Forces on Vertical Circular Cylinders", Journal of Waterways, Harbours and Coastal Engineering Division, ASCE, Vol 102, No WW 2, Proc Paper 12140, May, 1976, pp 203-221.
3. Fryer, D K, Gilbert, G, and Wilkie, M J, "Wave Spectrum Synthesizers", Tech Memo 1/1972, Electrical and Mechanical Engineering Section, Hydraulics Research Station, Wallingford, UK, June, 1972.
4. Gaster, M "Vortex Shedding from Slender Cones at low Reynolds Numbers", Journal of Fluid Mechanics, Vol 38, 1971, pp 565-577.
5. Isaacson, M de St Q and Maull, D J, "Transverse Forces on Vertical Cylinders in Waves", Journal of Waterways, Harbour and Coastal Engineering Division, ASCE, Vol 102, No WW1, Proc Paper 11934, February, 1976, pp 49-60.
6. King, R, Prosser, M J, and Verley, R L P "The Suppression of Structural Vibrations Induced by Currents and Waves", Proc BDSS Conf, Trondheim, 1976, pp 263-283.
7. Mair, W A and Stansby, P K "Vortex Wakes of Bluff Cylinders in Shear Flow" Proc of the Int Symp on Modern Developments in Fluid Dynamics, SIAM, 1977, pp 129-150.

8. Maull, D J and Milliner, M G "Sinusoidal Flow Past a Circular Cylinder" to appear in Coastal Engineering.
9. Miller, B L and Matten, R B "A Technique for the Analysis of Wave Loading Data Obtained from Model Tests", NPL Report Mar Sci R 136, London, June, 1976.
10. Sarpkaya, T and Tuter, O "Periodic Flow About Bluff Bodies - Pt 1: Forces on Cylinders and Spheres in a Sinusoidally Oscillating Fluid", Report No NPS-59SL74091, Naval Postgraduate School, Monterey, California, 1974.
11. Sarpkaya, T "Vortex Shedding and Resistance in Harmonic Flow About Smooth and Rough Circular Cylinders at High Reynolds Numbers", Report No NPS-59SL76021, Naval Postgraduate School, Monterey, 1976.
12. Stansby, P K "Base Pressure of Oscillating Circular Cylinders", Journal of Engineering Mechanics Division, ASCE, Vol 102, No EM4 Proc Paper 12311, August, 1976, pp 591-600.
13. Stansby, P K "An Inviscid Model of Vortex Shedding from a Circular Cylinder in Steady and Oscillatory Far Flows", Proc Institution of Civil Engineers, London, Vol 63, Pt 2, Paper 8065, December, 1977, pp 865-880.
14. Susbielles, G G, "Wave Forces on Pile Sections due to Irregular and Regular Waves", Proc 7th Offshore Technology Conference, Paper No 1006, Houston, 1971.
15. Warren, J G "The Development and Use of a Wave Facility to Investigate the Dynamic Response of Circular Cylinders to Wave Action", PhD Thesis, University of Salford, 1977.
16. Zdravkovich, M M and Namork, S E "Formation and Reversal of Vortices around Circular Cylinders Subjected to Water Waves", Journal of Waterway, Port, Coastal and Ocean Division, ASCE, Vol 103, No WW 3, Proc Paper 13102, August, 1977, pp 378-383.

APPENDIX II - Notation

C_D = drag coefficient in Morison equation

C_M = inertia coefficient in Morison equation

$C_L(t) = Y / \frac{1}{2} \rho U_o^2 D$ = non-dimensional lift force

$C_X(t) = X / \frac{1}{2} \rho U_o^2 D$ = non-dimensional in-line force

D = cylinder diameter

d = water depth

f_n = structural frequency

- f_w = wave frequency
 Fr = structural frequency/wave frequency
 $k=2\pi/L$ = wave number
 $KC=U_0T/D$ = Keulegan-Carpenter number (at surface)
 L = wavelength
 \bar{m} = equivalent mass/unit length
 $Re=\rho U_0D/\mu$ = Reynolds number (at surface)
 $S\eta$ = standard deviation at water surface elevation
 T = wave period
 U_0 = amplitude of horizontal water-particle velocity (linear theory)
 x_0 = in-line cylinder displacement
 y_0 = transverse cylinder displacement
 X = in-line force
 Y = lift force
 δ = logarithmic decrement of structural damping
 μ = viscosity of water
 ρ = density of water

Acknowledgements

This work was in part supported by the Research Department, Taylor Woodrow Construction Ltd and the Science Research Council, for which the authors express their appreciation. Thanks are also due to the staff of the Civil Engineering Department, University of Salford for their assistance both with the experiments and with the preparation of this paper.

Table 1. Parameter values for regular wave tests.

SERIES	A	B	C	D	E	F	G	H	I	J	K	L	M
D(mm)	21	28	28	28	36	36	36	36	54	54	36	36	28
$S\eta$ (mm)	40	40	40	40	40	40	40	40	40	40	30	45	30
$\bar{m}/\rho D^2$	17	48	32	19	38	24	16	12	27	20	24	24	48
$\delta \approx 0.2$ for all cases													